© creative

Scientific paper

A New Zn(II) Two-dimensional Coordination Polymer: Synthesis, Structure, Highly Efficient Fluorescence and DFT Study

Fen-Fang Li

Department of Chemistry and Chemical Engineering, Jinzhong University, Jinzhong, Shanxi 030600, China.

* Corresponding author: E-mail: lffspring@126.com

Received: 03-26-2022

Abstract

A new two-dimensional coordinate polymer, $\{[Zn_2(pbmpd)(H_2O)_4]\cdot(H_2O)\}_n$ ($H_4pbmpd=1,1$ '-(1,4-phenylenebis(methylene))bis-(1H-pyrazole-3,5-dicarboxylic acid)), has been hydrothermally synthesized and characterized by IR spectrum, elemental analysis, TGA and X-ray single-crystal/powder diffraction. Structural analyses reveal that complex 1 exhibits a two-dimensional sheet structure in the crystal lattice. In complex 1, the carboxylic oxygen atoms and conjugated N atoms of pbmpd⁴⁻ bridge zinc(II) ions form indefinitely zigzag shaped one-dimensional chains through $\pi\cdots\pi$ stacking interactions which are further connected by $[ZnO_6]$ units to form a novel two-dimensional structure. Finally, $\pi\cdots\pi$ stacking interactions and intermolecular hydrogen bonds assemble the two dimensional networks into a three-dimensional framework. Furthermore, the luminescent properties are also discussed. Interestingly, the solid state photoluminescence properties of the title polymer show the enhancement effect of spectrum. Density functional theory (DFT) calculations were used to support the experimental data.

Keywords: Zn(II) complex; crystal structure; 1,1'-(1,4- phenylenebis(methylene)) bis-(1H-pyrazole-3,5-dicarboxylic acid); fluorescence property; DFT study

1. Introduction

Luminescent metal–organic frameworks (LMOFs), as important functional crystalline materials, are gaining increasing attention in sensing applications during the past few years owing to their high sensitivity, short response time and their ability to be employed both in solution and the solid phase. ¹⁻³ Therefore, the synthesis of LMOFs is the basis of such work. LMOFs can be synthesized quickly and conveniently through self-assembly of π -conjugated multidentate organic bridging ligands with d^{10} metal ions or/and lanthanide metal ions. ^{4,5} Furthermore, such ligands also possess a better selective recognition ability, higher chemical and thermal stability and so on. ^{6,7}

Polycarboxylates based pyrazole as a kind of π -electron rich ligand, have great benefits for the formation 2D or 3D metal-organic frameworks (MOFs), some of these, which contain Zn²⁺/Cd²⁺ ions and/or clusters, often possessing good photoluminescence properties.^{8,9} Furthermore, rigid multicarboxylate ligands as bridging or building blocks play crucial roles in the construction of stable coordination frameworks, but their skeleton

structures are limited. In contrast, flexible multicarboxylate ligands have remarkable advantages because their conformational freedom and flexibility can be fine-tuned by themselves to match with the coordination preference of metal ions and lower the energetic arrangement in the self-assembly process. The synthesis of coordination polymers based on flexible multicarboxylate is also influenced by the chemical and structural features of organic ligands, metal-to-ligand ratio, the coordination geometries of the metal, pH value, temperature, solvent and so on. Among these factors, the key factor is the selection of the organic ligand, which determines the topology of the synthetic architecture through its excellent coordination capabilities and versatile bridging modes. Therefore, multifarious tetracarboxylate ligands have been utilized to create desired coordination polymers with fascinating frameworks and properties, such as 5,5'-(1H-1,2,3-triazole-1,4-divl)diisophthalic acid, 10 5,5'-(1,4-Phenylenebis(methylene) bis(oxy)di-isophthalic acid, 11 1,1'-bis(3,5-dicarboxybenzyl)-4,4'-bipyridinium dichloride,¹² 2,3,3',4'-diphenyl ether tetracarboxylic acid.13 To date, the coordination

polymers built from 1,1'-(1,4-phenylenebis(methylene)) bis(1H-pyrazole-3,5-dicarboxylic acid) have rarely been explored.^{14, 15}

Herein, we selected the ligand, 1,1′-(1,4-phenylenebis(methylene))bis(1H-pyrazole-3,5-dicarboxylic acid) (H₄pbmpd) which the four carboxyl groups linked by two flexible '-CH₂-' groups and two free N atoms offer ample coordination capacities and the ability to adapt its conformation to geometrical requirements leading to producing interesting structures with amazing properties and successfully synthesized a new 2D MOF, {[Zn₂(pbmpd) (H₂O)₄]·H₂O}_n. The synthesized samples were characterized by X-ray single-crystal and powder diffractions, thermal gravimetric analysis and infrared spectra. In addition, we have also discussed the photoluminescence mechanism via density functional theory (DFT) calculations.

2. Experimental

2. 1. Materials and Measurements

H₄pbmpd was purchased from Jinan Henghua Science & Technology Co. Ltd, China (Fig.1). All solvents and other reagents were commercially available and were used without further purification. The IR spectrum for complex 1 was recorded in a KBr pellet in the range of 4000~400 cm⁻¹ on a Bruker TENSOR27 spectrometer. Element analysis was carried out using a CHNO Rapid instrument. Powder X-ray diffraction (PXRD) data were collected on a Bruker D8 Advance with Cu $K\alpha$ radiation (λ = 1.5418 Å). The thermogravimetric analysis (TGA) was carried out with a Dupont thermal analyser in the temperature range of 293~1073 K under an N₂ atmosphere with a heating rate of 10 K min⁻¹.

Fig. 1. 1,1'-(1,4- Phenylenebis(methylene))bis-(1H-pyrazole-3,5-dicarboxylic acid, H₄pbmpd)

2. 2. Synthesis of $\{[Zn_2(pbmpd) (H_2O)_4] \cdot (H_2O)\}_n (1)$

A mixture of H_4 pbmpd (33.2 mg, 0.05 mmol), $Zn(NO_3)_2 \cdot 4H_2O$ (36.5 mg, 0.10 mmol) and a 12 mL of acetonitrile / water (2 : 10, V/V) was placed in a 15 mL of Teflon-lined stainless steel autoclave. The mixture was heated under autogenous pressure at 433 K for 72 h and then cooled to room temperature. Colourless block crystals were collected by filtration, washed with H_2O_3 and

dried in air. (yield: 75%, based on H_4pbmpd). Analysis calculated for $C_{18}H_{20}Zn_2N_4O_{13}$: C 34.33, H 2.86, N 8.90%; found: C 34.38, H 2.81, N 8.93%. IR (KBr, v, cm⁻¹, s for strong, m medium, w weak): 3416 m, 1594 s, 1534 s, 1485 s, 1431 m, 1349 s. 1289 m, 1208 w, 1131 m, 1023 s, 854 m, 794 s, 555 m.

2. 3. Crystal Structure Determination

Diffraction data were collected using a SuperNova (Cu) X-ray Source diffractometer utilizing Cu- $K\alpha$ (λ = 1.5418 Å) radiation at 173 K. The structure was solved by direct methods employed in the program SHELXS-2014, and refined by full-matrix leastsquares methods against F² with SHELXL-2016. ¹⁶ The cell parameters were determined by SMART software. Data reduction was performed with SAINT Plus. Program SADABS was used for absorption corrections. All non-H atoms were refined anisotropically, hydrogen atoms attached to C atoms were placed geometrically and refined using a riding model approximation, with C-H = 0.93 Å and $U_{iso}(H) = 1.2U_{eq}(C)$. H atoms bonded to O were located firstly in a difference Fourier map and were refined freely. Tentative free refinements of their positional coordinates resulted in an unsatisfactory wide range of O-H and H...H (in water) distances; bond lengths were therefore restrained to 0.82 (1) Å for O-H. The H...H (in water) distances were restrained to 1.32 (1) Å. The O-H distances of water molecules are in the range

Table 1. Crystal data and structure refinement for Complex 1

	1
Empirical formula	$C_{18}H_{20}Zn_2N_4O_{13}$
Formula weight	631.12
Temperature	173 K
Crystal system	monoclinic
Space group	$P2_1/c$
a / Å	a = 12.8594 (4)
b / Å	b = 14.7599(4)
c / Å	c = 11.4301 (4)
β / (°)	$\beta = 91.303(3)$
$V/Å^3$	2168.91 (1)
Z	4
Density (calculated)	1.933 mg/m^3
Absorption coefficient	3.477 mm ⁻¹
F(000)	1280
Crystal size	$0.20 \times 0.20 \times 0.10 \text{ mm}$ 3
θ range for data collection	2.7 to 26.5°
Reflections collected	8113
Independent reflections	$3951 [R_{int} = 0.029]$
Completeness to $\theta = 25.50^{\circ}$	96.7 %
Refinement method	Full-matrix least-squares on F^2
Data / restraints / parameters	3951/ 0/334
Goodness-of-fit on F^2	1.040
Final <i>R</i> indices $[I > 2\sigma(I)]$	$R_1 = 0.0306, wR_2 = 0.0819$
R indices (all data)	$R_1 = 0.0389, wR_2 = 0.0769$

Table 2. Selected Bond Lengths (Å) and Bond Angles (°) for Complex 1

1			
Zn(1)-O(9)	1.9886 (1)	Zn(1)-O(5)	2.0330 (1)
Zn(1)-N(1)	2.124(2)	Zn(1)-N(3)	2.065 (2)
Zn(2)-O(3)	2.119(2)	Zn(2)-O(4)	2.400(2)
Zn(2)-O(10)	2.0237 (1)	Zn(2)-O(11)	2.028 (2)
Zn(1)-O(1)	2.0185(1)	Zn(2)-O(7)	2.0815(1)
Zn(2)-O(12)	2.0888 (1)		
O(9)-Zn(1)-O(1)	88.35 (8)	O(1)-Zn(1)-O(5)	168.77 (8)
O(9)-Zn(1)-O(5)	88.63 (8)	O(9)-Zn(1)-N(3)	111.19 (9)
O(9)-Zn(1)-N(1)	145.25 (9)	O(5)-Zn(1)-N(1)	96.65 (8)
O(1)-Zn(1)-N(1)	79.85 (8)	O(1)-Zn(1)-N(3)	109.27 (8)
O(10)-Zn(2)-O(12)	93.91 (8)	O(7)-Zn(2)-O(12)	175.82 (8)
O(11)- $Zn(2)$ - $O(12)$	82.05 (8)	O(10)-Zn(2)-O(3)	141.17 (8)
O(10)-Zn(2)-O(4)	84.48 (7)	O(12)-Zn(2)-O(3)	93.05 (8)
O(7)-Zn(2)-O(4)	98.53 (7)	O(10)-Zn(2)-O(11)	104.55 (8)
O(10)-Zn(2)-O(7)	86.70 (8)	O(3)-Zn(2)-(4)	58.05 (8)
O(5)-Zn(1)-N(3)	81.90 (8)	N(3)-Zn(1)-N(1)	103.55 (8)
O(11)-Zn(2)-O(3)	114.24 (8)	O(7)-Zn(2)-O(3)	89.04 (8)
O(11)-Zn(2)-O(4)	165.16 (8)	O(12)-Zn(2)-O(4)	85.64 (8)
O(11)-Zn(2)-O(7)	93.79 (8)		

Table 3. Hydrogen Bond Lengths (Å) and Bond Angles (°) for Complex 1

D-H···A	d(D-H)	d(HA)	d(DA)	∠DHA
O(13)H(13B)···O(8) ^v	0.82	2.04	2.848 (3)	167
O(13)-H(13A)···O(6)	0.82	1.91	2.704(3)	162
C(13)-H(13)···O(9)vi	0.95	2.57	3.289 (3)	133
C(11)-H(11B)O(13)vii	0.99	2.50	3.388 (3)	149
C(11)-H(11A)····O(8) ^v	0.99	2.32	2.974(3)	122
C(4)-H(4B)-O(4)	0.99	2.33	2.981 (4)	123
$C(2)-H(2)\cdots O(4)^{i}$	0.95	2.30	3.246 (3)	171
O(12)-H(12B)···O(2)viii	0.82	1.96	2.746 (3)	160
O(12)-H(12A)···O(2) ⁱⁱⁱ	0.82	1.91	2.715 (3)	167
O(11)-H(11D)O(1)viii	0.82	1.94	2.735 (3)	162
O(11)-H(11C)····O(13)ix	0.82	1.90	2.690(3)	163
O(10)-H(10B)···O(3) ⁱⁱⁱ	0.82	2.15	2.949 (3)	167
$O(10)-H(10A)-O(6)^{ix}$	0.82	1.85	2.654(3)	169
$O(9)-H(9B)-O(8)^{x}$	0.82	1.96	2.731(3)	157
$O(9)-H(9A)\cdots O(7)^{xi}$	0.82	1.95	2.767 (3)	172
Cg1···Cg1 ^{vi}			4.117(1)	
Cg1Cg2			3.582(1)	
C(6)-H(6)···Cg3	0.95	2.95	3.665 (3)	130
$C(4)$ – $H(4A)$ ••• $Cg3^{xi}$	0.99	2.86	3.479 (3)	124

Symmetry codes: (i) x, -y+1/2, z-1/2; (iii) x, -y+1/2, z+1/2; (v) x-1, -y+1/2, z+1/2; (vi) -x, -y+1, -z+1; (vii) -x, y-1/2, -z+3/2; (viii) -x+1, y-1/2, -z+1/2; (ix) -x+1, y-1/2, -z+1/2; (xi) -x+1, -y+1, -z+1.

0.8199~0.8205 Å. A summary of the crystallographic data, data collection and refinement parameters for complex 1 is provided in Table 1. Selected bond lengths, bond angles and H-bonds for complex 1 are listed in Tables 2 and 3, respectively. The molecular graphics were prepared using the SHELXL-2016 and MERCURY programs.^{17,18}

2. 4. Hirshfeld Surface Analysis

The Hirshfeld surface analysis 19 and the related 2D-fingerprint plots 20 were calculated using Crystal Explorer. 21 The CIF file of the structure 1 was imported into Crystal Explorer and high resolution Hirshfeld surfaces were mapped with the function $d_{\rm norm}$. Then, the Hirshfeld surfaces were resolved into 2D-fingerprint plots, in order to quantitatively determine the nature and type of all intermolecular contacts experienced by the molecules in the crystal.

3. Results and Discussion

3. 1. IR Characterization

The peaks of FT-IR point out that the strong band around 1522 cm⁻¹ resulting from stretching vibration of carboxyl (C=O) in the free ligand is disappeared and splitted into two new bands at 1594 cm⁻¹ and 1534 cm⁻¹ in complex 1, which are assigned to symmetric and asymmetrical stretching vibrations of carboxyl (C=O). It suggests that the carboxyl of the ligand had been deprotonated and coordinated to the Zn(II).²² Complex 1 also shows broad absorptions in the range between 3416 cm⁻¹ associated with hydrogen-bonded O-H stretching vibration.²³

3. 2. Crystal Structure of Complex 1

The two-dimensional coordinate polymer 1 crystallizes in the $P2_1/c$ space group of the monoclinic crystal system and shows a 2D structure. The asymmetric unit of 1 contains two independent Zn^{2+} ions, one deprotonated pbmpd⁴⁻ ligand, four coordinated water molecules

and one solvent water molecule. As depicted in Fig. 2, the Zn(1) and Zn(2) centers exhibit different coordinated environments. Zn(2) exhibits distorted hexa-coordinated environments with one monodentate oxygen atom from the pbmpd⁴⁻ ligand (Zn(2)-O(7)), two chelating oxygen atoms originating from another pbmpd4- ligand (Zn(2)-O(3) and Zn(2)-O(4)) and three oxygen atoms (Zn(2)-O(10), Zn(2)-O(11) and Zn(2)-O(12)) derived from the coordinated water molecules. The Zn-O coordination distances range from 2.081 (18) to 2.398 (2) Å which are all within the normal ranges.^{24–26} Zn(1) is penta-coordinated and displays a square pyramid ZnN₂O₃ geometry which is coordinated by three oxygen atoms (O(9), O(5) and O(1)) and two nitrogen atoms (N(1) and N(3)). The O(9) atom is from a terminal coordinated water molecule and O(1) and O(5) oxygen atoms are from monodentate carboxylate groups of pyrazole-carboxylate units from two different ligands. Two monodentate pyrazole nitrogen atoms (N(1)) and N(3) are derived from the two ligands. The Zn-O coordination distances range from 1.935 (7) to 2.204 (16) Å and Zn-N coordination distances range from 2.075 (4) to 2.139 (4) Å, which are also observed in reported zinc compounds.^{27, 28} Atoms O(9), O(5), O(1) and N(1), which are nearly coplanar (the mean deviation from the common best plane is 0.147 Å), complete the square base plane, while the vertex is occupied by atom N(3) of which the distance to the square plane is 2.392 (2) Å. The selected bond lengths are listed in Table 2.

In the structure of 1, the carboxylic oxygen atoms and conjugated N atoms bridge Zn(1) ions form an indefinitely zig-zag shaped 1D Zn(1) chains along the c axis through $\pi \cdots \pi$ stacking interactions between the ring Cg1 (N(3)/N(4)/C(12)-C(14)) and the ring Cg2 (C(5)-C(10))with the centroid distance of 3.582 (1) Å and the Zn···Zn distance is 11.43 Å (Fig. 3). Meanwhile, the Zn(1) chains are further connected by [Zn₂O₆] units to form a novel 2D structure (Fig. 4). The $\pi \cdots \pi$ stacking interaction between the adjacent rings Cg1 (N(3), N(4), C(12), C(13), C(14)) and Cg1i with the centroid distance of 4.117 (1) Å, lead to a weak interconnection of these layers into a three-dimensional (3D) framework. This type of self-assembled dimers has been studied in Cd(II) complex with the similar ligand. ²⁹ In addition, $C(6)-H(6)\cdots Cg3$ (N(1)/N(2)/C(1)-C(3))and C(4)-H(4A)···Cg3ii interactions (see Fig. 5), with distances of 2.86 Å and 2.95 Å respectively, are also found to stabilize the 3D network.

There are interesting strong O–H···O hydrogen bonds among the rich carboxyl molecules. Viewing along *bc* plane, inter-molecular hydrogen bonds among carboxylate from pyrazole-carboxylate and coordinated water molecules O atoms, named O(13)–H(13B)···O(8)ⁱ, O(12)–H(12B)···O(2)^{vii}, O(13)–H(13A)···O(6), O(9)–H(9B)···O(8)^{viii}, O(9)–H(9A)···O(7)^{ix}, O(10)–H(10B)···O(3)^{vi}, O(12)–H(12B)···O(2)^v connect the two-dimensional coordination network into a three-dimensional framework (Fig. 6). Interatomic distances ranging from 0.2654 (3) to 2.949

(3) Å and angles within 157.4~172.4° indicated strong hydrogen bonds. Meanwhile the intra-molecular hydrogen bonds named O (13)–H (13A)···O(6) with the distance is 2.704 (3) Å is also been found to strengthen the network. The detailed hydrogen bonds are listed in Table 3.

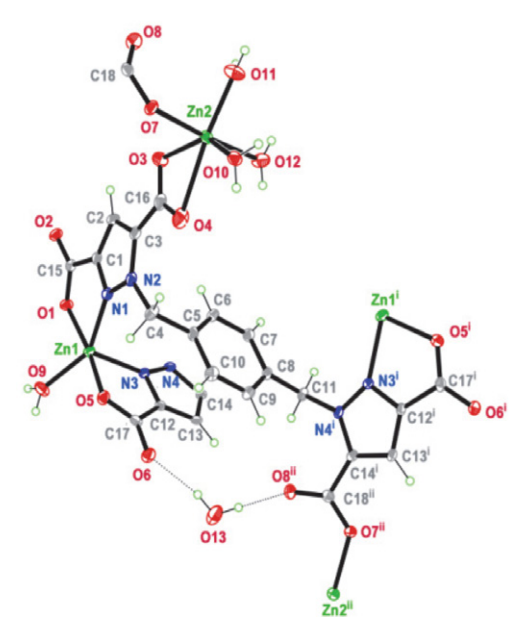


Fig.2. The atom labels and coordination environments of the Zn(II) ions in complex 1, with displacement ellipsoids drawn at the 30% probability level. Dashed lines represent hydrogen bonds.

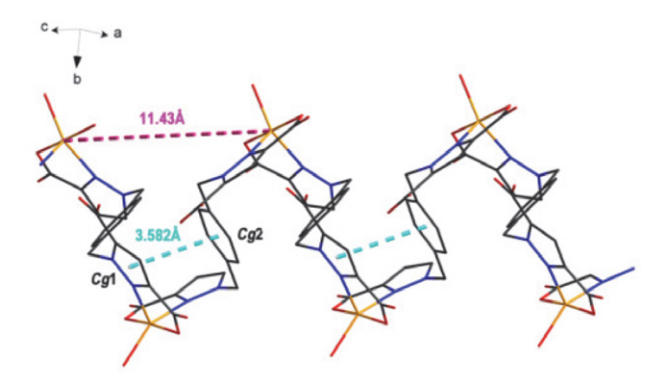


Fig. 3. The infinite one-dimensional zigzag shaped chain formed from Zn(2) atoms and pbmpd⁴⁻ ligands through p··· π stacking interactions (blue dashed lines) along the c axis.

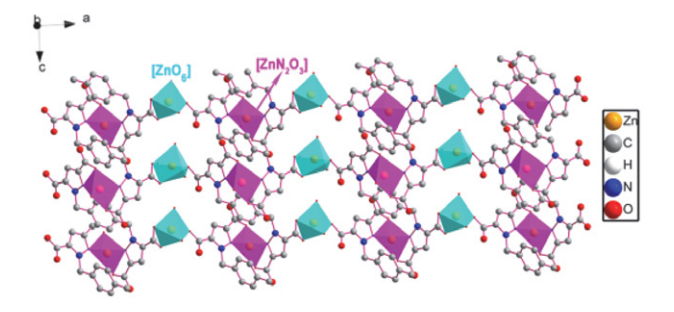


Fig. 4. The two-dimensional sheets extending in the *ac* plane formed by layers packed through with $[ZnO_6]$ and $[ZnN_2O_3]$ units.

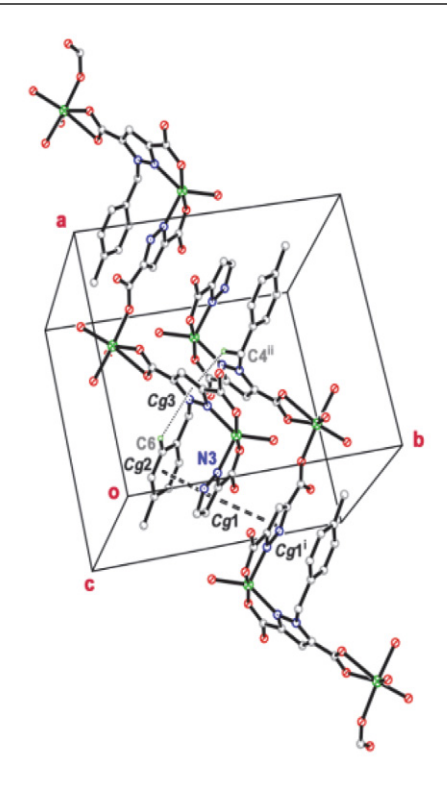


Fig. 5. $\pi \cdots \pi$ stacking interactions (open dashed lines) and C-H··· π interactions (dashed lines) present in complex 1.

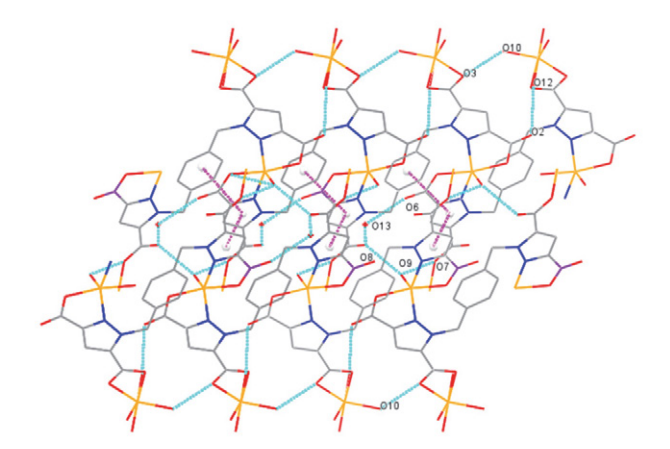


Fig. 6. The three-dimensional network through $\pi \cdot \cdot \cdot \pi$ stacking interactions (purple lines) and inter-molecular hydrogen bonds (blue lines) viewing along ac plane. White balls represent the centroid of the rings. (Symmetry codes: (i) x - 1, -y + 1/2, z + 1/2; (v) -x + 1, y - 1/2, -z + 1/2; (vi) x, -y + 1/2, z + 1/2; (vii) -x + 1, y - 1/2, -z + 3/2; (viii) -x + 1, y + 1/2, -z + 1/2; (ix) -x + 1, -y + 1, -z + 1.)

3. 3. Hirshfeld Surface Analysis

The intermolecular interactions in crystal structure 1 were quantified using Hirshfeld surface analysis and fingerprint plots (FP). The dominant intermolecular interactions are viewed as a bright red area on the d_{norm} surface. Fig. 7 illustrates samples of Hirshfeld surfaces for structure 1. In 1, we observe a high level of O···H interactions due to

the hydrogen bonds between solvents molecules and the complex. The two-dimensional fingerprint plots for complex 1 are shown in Fig.8. The proportions of C–H··· π , π ··· π and O–H···O interactions are 11.2%, 8.8% and 39.6% of the total Hirshfeld surfaces for complex 1. It appears that in this complex rich in aromatic rings, contact characteristics of π -stacking or C–H/ π interactions are less important.

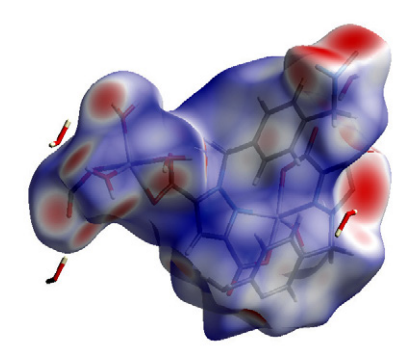
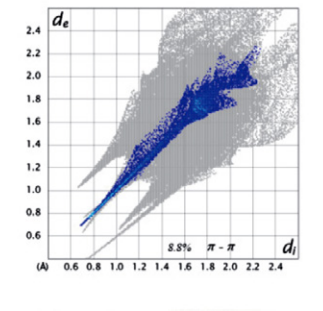
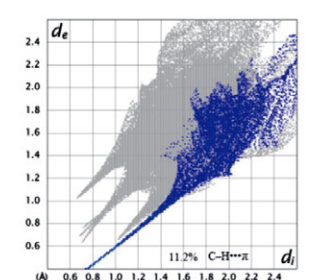


Fig.7. Views of the Hirshfeld surfaces for 1 mapped with d_{norm} .





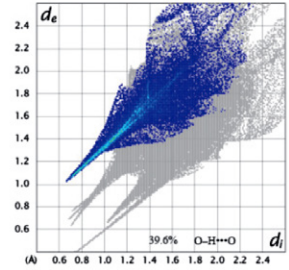
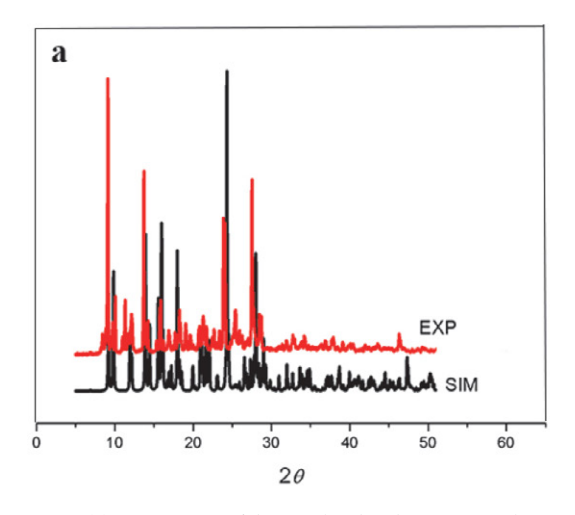


Fig. 8. Fingerprint plots of complex 1: $C-H\cdots\pi$, $\pi\cdots\pi$ and $O-H\cdots O$, listing the percentages of contacts contributed to the total Hirshfeld surface area of molecules.

3. 4. PXRD and TG Analyses

To confirm that the phase of the bulk sample is pure and the crystal structure of complex 1 is truly representative of the bulk material, a powder X-ray diffraction (PXRD) experiment was carried out on a Bruker D8 Advance with Cu $K\alpha$ radiation (λ = 1.5418 Å). The as-synthesized sample of 1 is characterized by powder X-ray diffraction (PXRD). As shown in Fig. 9a, the PXRD patterns are almost consistent with the simulated spectrum, demonstrating the high phase purity of the compounds.

As shown in Fig. 9(b), the TGA for complex 1 shows a weight loss of 12.1% (calculated 14.2%) between 293 K and 605 K, which is associated with the loss of one solvent



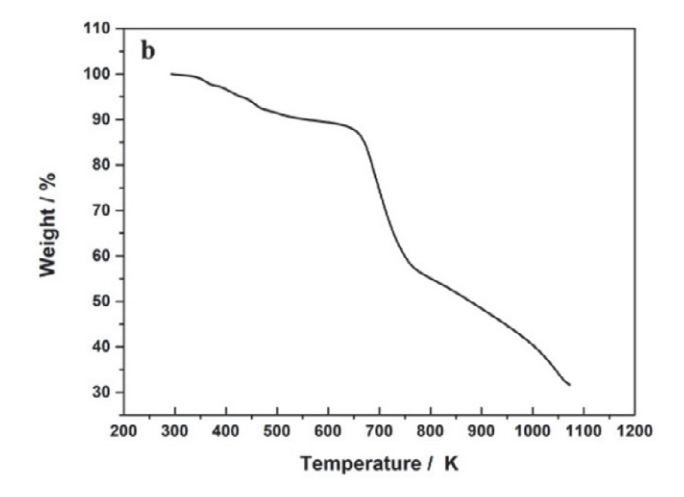


Fig. 9. (a) Comparison of the simulated and experimental PXRD patterns of complex 1. (b) Thermogravimetric analysis (TGA) curve of complex 1

water molecule and four coordinated water molecules. When the temperature is up to 646 K, the frameworks of complex 1 begin to break down gradually.

3. 5. Fluorescence Properties and DFT Calculation

The luminescent properties of complex 1 and free ligand were examined in the solid state at room temperature. As depicted in Fig. 10, the emission of free H₄pbmpd is weak, whereas complex 1 reveals an obviously strong emission; and the maximum emission of 1 at ca. 448 nm has a blue shift compared with that of the free H₄pbmpd ligand observed at $\lambda_{\rm em}$ = 495 nm ($\lambda_{\rm ex}$ = 300 nm). In order to obtain a better insight into the nature of the photoluminescence of complex 1, we investigated the structural, electronic and optical properties with S₀ using DFT calculations at the B3LYP/6-31+G* level of the Gaussian 09 program and S₁ using TD-DFT calculations at the B3LY-P/6-31+G* level of the Gaussian 09 program. 30 The geometry was taken from the crystal structure. According to Kasha's rule, 31 the fluorescence of the compounds is only emitted from the lowest singlet excited states (S₁) to the singlet ground state (S_0) . As depicted in Fig. 11, for complex 1, in the S₁ state, the HOMO is located more on the π orbitals of the pyrazole-carboxylate moiety of the ligand, and the LUMO is mainly located on the π^* orbital of the pyrazole-phenyl moiety. Obviously, the LUMO and HOMO orbits of complex 1 are both distributed over the ligand, and their emission bands can thus be clearly assigned to the ILCTs. Meanwhile, the HOMO-LUMO energy gap of compound 1 is larger than that of the free ligand, which leads to the blue shift of the emission peak (47 nm) compared with the free H₄pbmpd ligand, indicating that the HOMO-LUMO energy gap decreases to make the blue shift, as reported for other pyrazole derivated polycarboxylate complexes.³² The enhanced emission intensity of complex 1 may arise from the aggregation in-

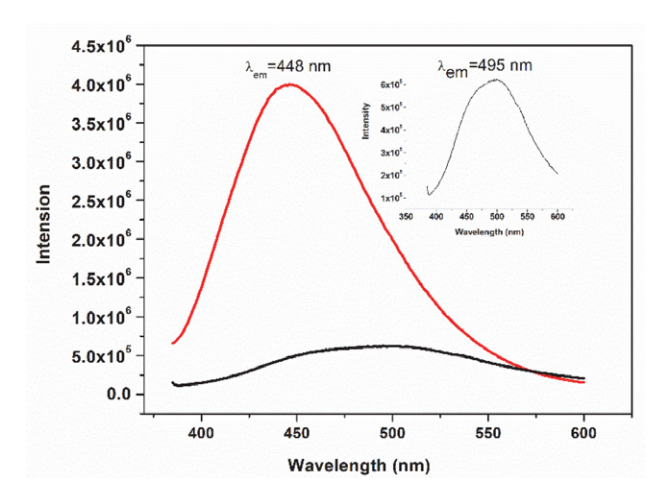


Fig. 10. Solid-state emission spectra of H₄pbmpd (black) and complex 1 (red) at room temperature (inset: enlarged view of emission spectra of H₄pbmpd).

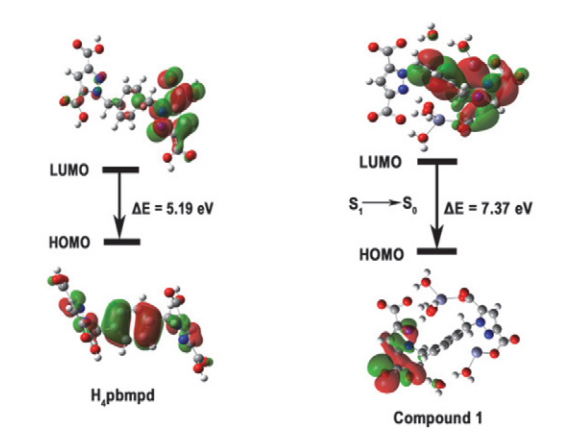


Fig. 11. The frontier MOs and the DFT calculations of $\rm H_4pbmpd$ ligand and complex 1.

duced emission, where the coordination of the ligand and the metal ions can reduce the freedom of the ligands and their non-radiative transitions. ^{33,34}

4. Conclusion

A new $2D \operatorname{Zn}(II)$ compound based on 1,1 ´-(1,4-phenylenebis(methylene))bis- (1H-pyrazole-3,5-dicarboxylic acid) has been constructed successfully. Complex 1 is consisted of two independent $\operatorname{Zn^{2+}}$ ions but have different coordinated environments, one of which exhibits distorted hexa-coordinated environments, while the other displays a square pyramid $\operatorname{ZnN_2O_3}$ geometry. In complex 1, the indefinitely zig-zag shaped $\operatorname{1D}$ chains formed by the ligand pbmpd⁴⁻ bridged Zn ions and $[\operatorname{Zn_2O_6}]$ units to form a $\operatorname{2D}$ structure. In addition, compared to the ligand, the solid state photoluminescence properties of complex 1 show an obviously strong emission, which is assigned to the ILCTs by Density functional theory (DFT) calculations.

Supplementary Material

CCDC 1923324 contains the supplementary crystal-lographic data for this paper. These data can be obtained free of charge from The Cambridge Crystallographic Data Centre via http://www.ccdc.cam.ac.uk/conts/retrieving.html.

Acknowledgments

Authors appreciated the Startup Fund of Doctors of Jinzhong University. A portion of this work was performed on the Scientific Instrument Center of Shanxi University of China.

6. References

- M. Pan, W. M. Liao, S.Y. Yin, S.S. Sun, C.Y. Su, Chem Rev 2018, 118, 8889–8935; DOI:10.1021/acs.chemrev.8b00222
- H. Y. Li, S. N. Zhao, S. Q. Zang, J. Li, Chem Soc Rev 2020, 49, 6364–6401; DOI:10.1039/C9CS00778D
- X. Y. Liu, W. P. Lustig, J. Li, Chem. Rev 2020, 5, 2671–2680;
 DOI:10.1021/acsenergylett.0c01148
- Y. W. Li, J. Li, X. Y. Wan, D. F. Sheng, H. Yan, S. S. Zhang, H. Y. Ma, S. N. Wang, D. C. Li, Z. Y. Gao, J. M. Dou, D. Sun, *Inorg. Chem* 2021, 60, 671–681;
 - DOI:10.1021/acs.inorgchem.0c02629
- W. B. Liu, N. N. Li, X. Zhang, Y. Zhao, Z. Zong, R. X. Wu, J. P. Tong, C. F. Bi, F. Shao, Y. H. Fan, *Cryst. Growth Des* 2021, 21, 5558–5572; DOI:10.1021/acs.cgd.1c00359
- A. Mukhopadhyay, S. Jindal, G. Savitha, J. N. Moorthy, *Inorg. Chem* 2020, 59, 6202–6213;
 - DOI:10.1021/acs.inorgchem.0c00307
- F. Y. Yi, M. L. Gu, S. C. Wang, J. Q. Zheng, L. Q. Pan, L. Han, Inorg. Chem 2018, 57, 2654–2662;
 - DOI:10.1021/acs.inorgchem.7b03053
- W. Q. Tong, W. N. Liu, J. G. Cheng, P. F. Zhang, G. P. Li, L. Hou, Y. Y. Wang, *Dalton Trans* 2018, 47, 9466–9473;
 DOI:10.1039/C8DT01694A

- C. Feng, Y. H. Ma, D. Zhang, X. J. Li, H. Zhao, *Dalton Trans* 2016, 45, 5081–5091; DOI:10.1039/C5DT04740D
- L. B. Sun, Y. Li, Z. Q. Liang, J. H. Yu, R. R. Xu, *Dalton Trans* 2012, 41, 12790–12796; DOI:10.1039/c2dt31717f
- 11. X. He, X. P. Lu, M. X. Li, R. E. Morris, *Cryst. Growth Des* **2013**, *13*, 1649–1654; **DOI**:10.1021/cg3018562
- L. K. Li, H. Y. Li, Li Ting, L. H. Quan, J. Xu, F. A. Li, S. Q. Zang, CrystEngComm 2018, 20, 6412–6419;
 DOI:10.1039/C8CE01335G
- Q. Yue, Y. Y. Wang, X. L. Hu, W. X. Guo, E. Q. Gao, Cryst-EngComm 2019, 21, 6719–6732; DOI:10.1039/C9CE01128E
- 14. Y. P. Xia, Y. W. Li, D. C. Li, Q. X. Yao, Y. C. Du, J. M. Dou, *Cryst-EngComm* **2015**, *17*, 2459–2463; **DOI**:10.1039/C5CE00162E
- F. F. Li, M. L. Zhu, L. P. Lu, A. Wang, Journal of Solid State Chemistry 2020, 290, 121582–121590;
 DOI:10.1016/j.jssc.2020.121582
- G. M. Sheldrick, SHELXS-97, Program for X-ray Crystal Structure Solution. University of Göttingen, Germany 1997.
- 17. Mercury 2.3 Supplied with Cambridge Structural Database, CCDC, Cambridge, U.K. **2003–2004**.
- L. Y. Zhang, L. P. Lu, M. L. Zhu, Chin. J. Struct. Chem 2018, 37, 427–436; DOI: 10.14102/j.cnki.0254-5861.2011-1752
- M. A. Spackman, D. Jayatilaka, CrystEngComm 2009, 11, 19–32; DOI:10.1039/B818330A
- M. A. Spackman, J. J. McKinnon, CrystEngComm, 2002, 4, 378–392; DOI:10.1039/B203191B
- S. K. Wolff, D. J. Grimwood, J. J. McKinnon, M. J. Turner, D. Jayatilaka, M. A. Spackman, CrystalExplorer (Version 3.1), University of Western Australia, 2012.
- 22. Q. K. Zhou, N. Y. Li, *Acta Cryst* **2017**, *C73*, 749–753; **DOI**:10.1107/S2053229617012189
- G. M. Sheldrick, Acta Crystallogr. Sect C 2015, 71, 3–8;
 DOI:10.1107/S2053229614024218
- 24. Y. Y. An, L. P. Lu, M. L. Zhu, *Chin. J. Struct. Chem* **2018**, *37*, 1479–1485; **DOI:** 10.14102/j.cnki.0254-5861.2011-1945
- Y. M. Zhang, S. Yuan, G. Day, X. Wang, X. Y. Yang, H. C. Zhou, *Coord. Chem. Rev* 2018, 354, 28–45;
 DOI:10.1016/j.ccr.2017.06.007
- W. Yang, C. M. Wang, Q. Ma, X. N. Feng, H. L. Wang, J. Z. Jiang, Cryst. Growth Des 2013, 13, 4695–4704;
 DOI:10.1021/cg4007372
- 27. X. Q. Yao, G. B. Xiao, H. Xie, D. D. Qin, H. C. Ma, J. C. Liu, P. J. Yan, *CrystEngComm* **2019**, *21*, 2559–2570; **DOI**:10.1039/C8CE02122H
- 28. M. Y. Liu, H. Y. Yu, Z. L. Liu, *CrystEngComm* **2019**, *21*, 2355–2361; **DOI**:10.1039/C9CE00034H
- F. F. Li, M. L. Zhu, L. P. Lu, Acta Cryst 2018, C74, 967–973;
 DOI:10.1107/S2053229618010239
- 30. M. J. Frisch, GAUSSIAN09. Gaussian Inc., Wallingford, CT, USA **2009.**
- 31. M. Kasha, *Discuss. Faraday Soc* **1950**, *9*, 14–19; **DOI**:10.1039/df9500900014
- 32. B. Roy, S. Mukherjee, P. S. Mukherjee, *CrystEngComm* **2013**, *15*, 9596–9602; **DOI:**10.1039/c3ce41080c
- 33. S. D. Li, L. P. Lu, M. L. Zhu, *CrystEngComm* **2018**, *20*, 5442–5456; **DOI**:10.1039/C8CE00947C

 J. J. Shen, M. X. Li, Z. X. Wang, Cryst.Growth Des 2014, 14, 2818–2830; DOI:10.1021/cg500092t

Povzetek

Sintetizirali smo nov dvodimenzionalni koordinacijski polimer, $\{[Zn_2(pbmpd)(H_2O)_4]\cdot(H_2O)\}_n$ $(H_4pbmpd = 1,1'\cdot(1,4-fenilenbis(metilen))bis\cdot(1H-pirazol-3,5-dikarboksilna kislina))$ in spojino karakterizirali z IR spektroskopijo, elementno analizo, TGA in rentgensko monokristalno/praškovno difrakcijo. Strukturna analiza je pokazala, da ima spojina 1 dvodimenzionalno plastovito strukturo. V strukturi spojine 1 karboksilatni kisikovi atomi in kojugirani N atomi iz pbmpd⁴⁻ povezujejo preko p··· π interakcij cinkove(II) ione v enodimenzionalne verige, ki so nadalje povezane preko $[ZnO_6]$ enot v dvodimenzionalno strukturo. Dvodimenzionalne strukture so preko p··· π interakcij in intermolekularnih vodikovih vezi nadalje povezane v tridimenzionalno mrežo. Raziskali smo luminiscenčne lastnosti produkta, pri čemer je zanimivo, da fotoluminiscenca v trdnem stanju kaže povečanje učinka spektra. Za podporo eksperimentalnim podatkom smo uporabili izračune DFT.



Except when otherwise noted, articles in this journal are published under the terms and conditions of the Creative Commons Attribution 4.0 International License